Journal of Ovonic Research Vol. 19, No. 1, January – February 2023, p. 87 - 103

The development of Ultra-high Aluminium graphene metal matrix composites (MMC) and improved the thermo-mechanical properties

M. Velliangiri*, M. Karthikeyan*, G. Sureshkannan*
Coimbatore Institute of Technology- Coimbatore – 14, India

Powder metallurgy has made it easier to develop Ultra high Al-Gr (5 wt% Gr) composite materials for commercial solar thermal collectors. This work seeks an optimum aluminum-graphene composite with superior thermo-mechanical properties for the thermal collector. Experimentally found that an AMMC matrix with 1.0 wt% of Gr has 282 W/mK thermal conductivity, 129 percent developed than Al (123 W/mK), and also found Al+Gr has a lower thermal expansion coefficient than pure Al. Predicted different composite densities and focused to retain 96.5 percent of aluminum density after sintering. Investigated analytical techniques and included some investigation like Raman spectroscopy, X-ray diffraction, FESM, and electricity-dispersive X-ray grain size and property and also identified high-quality composites and predicted their homogeneity and invulnerability. Predicted suitable Sintering temperature was 626 degrees Celsius which increased from 300 degrees Celsius. Energy and thermal conductivity were found that increases with increasing temperature and compared to pure Al. According to this investigation, when increased the graphene weight percentage proportion from 0 to 5.0 wt%. Results show that conductivity increases from 210 to 412 W/mK and mechanical characteristics slightly drop from 16 to 19% as pH rises from 5 to 5.5. Based on this investigation Al+Gr composites may be used for solar thermal collectors and heat sinks and also appropriate ultra-high Al+5.5 wt% suitable for solar collectors.

(Received February 24, 2022; Accepted February 3, 2023)

Keywords: Aluminium-graphene nanocomposites, Thermal conductivities, Thermal expansion properties, Vacuum sintered method, X-ray diffraction analysis, the study of Raman spectroscopy

1. Introduction

Many thermal applications and components may benefit from Aluminium Graphene MMC's heat conductivity and mechanical properties. Examples of composites' usefulness include thermoelectric sinks, heat sinks for tiny microelectronic devices, and high-performance thermo-mechanical device architectures. To get the best possible outcomes when creating novel applications using metal matrix composites (MMC), it is necessary to monitor, predict, and optimize powder (nanoparticles) size[1]. So, the weight % of the composite material may be affected by its conductivity, mechanical qualities, and characteristics[1, 2]. Certain physical and chemical features of the predicted necessary wt% of Gr were offered by research, such as dispersed phase and metal matrix interactions, into the finished composite combinations. It was shown that Bulk metallic matrices, which were predicted using MMC, exhibit both isotropic and anisotropic scattering properties [7, 8]. [3]. According to the author, recent funding has gone toward developing better thermo-mechanical properties and transportation infrastructure, as well as solar collector and heat sink technologies[2]. Thermo-mechanical properties of aluminium graphene composites are developed using the AMMC method, with help from determining the optimal Al-Gr wt% [4]. Although graphite is a superior particle to use for creating composites for

* Corresponding authors: velliangiri.m@cit.edu.in
https://doi.org/10.15251/JOR.2023.191.87

MMC, aluminium has the advantages of being lightweight and an excellent heat conductor (second only to copper). Aluminum with other metal nanoparticles causes major issues when building tribological structures compared to graphene composites. Although AMMC enhances the thermal conductivity of a variety of nanoparticles, including Al2O3, silicon carbide, boron nitride (BN), titanium boride (TiB2), boron carbide (B4C), and others, Al+Gr composites exhibit distinctive properties [5][6]. The authors discovered that cutting-edge research and development in the fields of nanomaterials and composites has helped to enhance these materials' electric, thermal, and tensile properties while also lowering their production costs. The chemical and thermal balance of Al+Gr, as well as carrier mobility, are crucial properties of graphene [1], which is used in airplane components. Strengthening metal matrix composites using graphene could be a good idea (MMC). To improve thermal conductivity, a nanostructured particle has been discovered and is deemed essential for even basic applications such as heat sinks [7][8][9]. Al+Gr is a composite/mixture of aluminium and graphene, which has been shown to have efficient heat transport and is critical for strength [2]. Preparing graphene nanoparticles, which can be used to extract high-quality Graphites, is also quite inexpensive. The author observed that AMMCs were more dispersed and had stronger interfacial interactions with graphene composite [2,10,7]. Dispersion research improved the MMC matrix and distributed phase amalgamation. Powder metallurgy beats high-energy ball-milling for developing metal powders because it avoids dispersion phase agglomeration. This work disperses graphene (reduced graphene oxide) particles to enhance MMC [2][11]. This composite has 125% higher thermal conductivity, 35% higher micro-hardness and 5% higher thermal expansion than pure aluminium. This research reveals that Aluminium +Gr heat exchangers maintain excellent thermophysical features, including conductivity and rapid heat absorption, which are helpful for hybrid MMCs and improved solar thermal (heat) collectors and feat sinks[1].

2. Materials and methodlogy

Metal-matrix composites (MMCs) necessitated this procedure because of their many practical applications; these properties include high strength, high-temperature resistance, a low melting point, and strong bonds. To put it another way, multi-material components help bring cutting-edge technologies like AMMC to market. Graphene composites are made with varying weight percentages using commercially available 99.9% aluminium powder. The manufacturing process included materials and methods that helped guarantee powder purity and toluene as quality control agents. The several techniques and graphene bands detected and also concentrated on to build the composites samples [1,12,3] are shown in Figures 1, 2, and 3(b). All Al-Gr composites have a density of 97.5 percent when sintered, which is the same as that of pure aluminium [1]. Sintered AlGr - 0.25 wt% of Gr material had an average hardness of 41 VHN, whereas sintered pure aluminium had an average hardness of 36 HV [1]. The approach aids in developing the samples and finding the inspections from the edge to the center of the specimen. Figure 4 depicts the investigation's key results (d). nanocomposites containing 0.25–0.5% graphene may boost micro-hardness [1, 14]. Results using atomic force microscopy characterization (AMMC) reveal that microhardness and strength improve with increasing graphene weight percent [1, 4].]. Metal matrix composites (MMCs), dislocations, and vacancies that can be trapped by graphene and prevented from propagating were the primary research targets. Graphene may also be used to fill empty spaces. Therefore, a greater amount of graphene in the aluminium matrix results in a lower microhardness [1, 15, 16]. The fact that graphene can fix broken grain edges [1] implies it may be able to stop grains from developing altogether. Figure 2 depicts the results together with their associated error bars. A linear pellet sample was heated and cooled in a sample container [1]. The size of the sample was 50 mm in diameter and 60 mm in thickness. As can be seen in fig.1, the sintered sample was tested in an argon atmosphere to make sure the thermocouple was giving accurate temperature measurements.

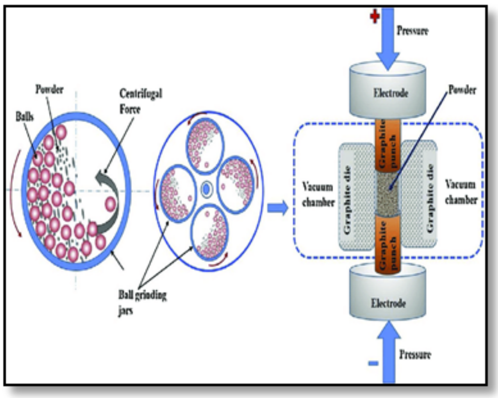

a)

b)

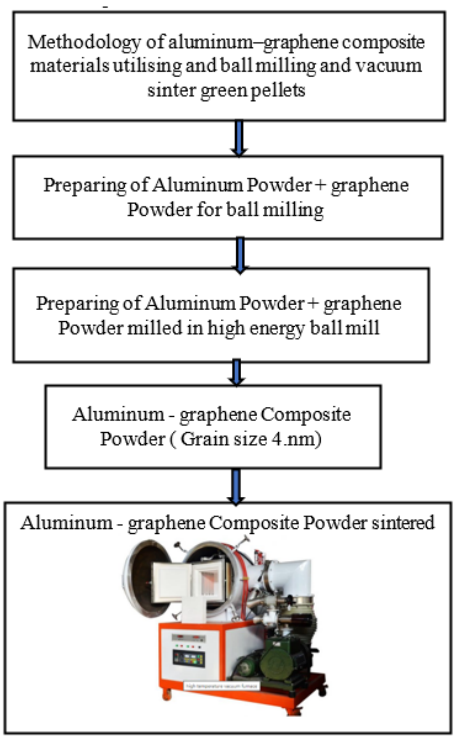

c)

Properties of Graphene powder	
Properties (Gr)	Value
Bond Type	sp^2
Layer number	Single Layer
Crystal structure	Hexagonal
Dimension	2D
Purity Degree (%)	99
Mass (bulk) density (g/cm^3)	~0,3
Absolute Density (g/cm^3)	2,25
Thickness (nm)	~1-2
Surface Area (m^2/g)	2600
High-Temperature Resistivity	−75 + 200 °C between not changing
Thermal Conductivity (WK^{-1}/m)	4840-5300
Electron Mobility cm^2 /(V.s)	$\sim 2,5 \times 10^5$
Elasticity Module (TPA)	~1

d)

Fig.1. Al+Gr Composites preparation in Vacuum Sintering and properties of Gr:
a) Al+Gr Composites preparation in Vacuum Sintering, b)Thermal Conductivity Apparatus, c)Methodology and Methods for creating nanocomposite of Al+Gr, d)Properties of Graphene powder.

Figure 1 shows the AL+Gr composite's Preparation methods and sintering and Properties. A substance's ability to withstand heat is determined by its thermal conductivity and expansion coefficient, hence a technique was created to improve both properties [1]. This coefficient, the parameters of which are shown in the figure, is dependent on the nature of the composite, its parts, and the circumstances in which the composite is operated [1]. The binding strength of both materials reduces as temperature rises [1],[11]. In many applications, the superior mechanical and thermal properties of metal matrix composites (MMCs) have led to their development as a methodology. High-performance mechanical structures, microelectronic devices, and thermoelectric materials all make advantage of MMCs. The composite may be affected by the sample's portion, size, shape, and orientation [5],[6]. Physical and chemical properties of the composite material may be altered at the interfaces between the dispersed phases and the metal matrix[7],[8]. The production and characteristics of an aluminium graphene composite are shown in Figures 1a–d. To accomplish certain goals, the MMC's distributed phase might be either isotropic or anisotropic. Production of airplanes, automobiles, electrical equipment, and building supplies all make use of composites [1]. These green pellets originated as milled graphene-aluminum composite powders [1, 2]. The supplies for sample preparation were packed down to a 128-ton load and 2.56-ton freight. Table 1 displays the characteristics of Al+Gr composites [1, 18].

Table 1. Thermal conductivity(K) evaluation between metals, Gr–epoxy, and Gr–metal composites.

Property	**Al**	**1.52wt%Gr**	**2.52wt%Gr**	**3.52wt%Gr**	**4.52wt%Gr**	**5.52wt%Gr**
Melting point(MP), ^{0}C	667	662	659	652	633	641
Density (, g·cm	4.75	2.64	2.45	2.35	2.31	2.15
HV 2000 mH	18.2	45.38	57.18	69.14	81.22	92.3
Elastic modulus, GPa	27.3	83.1	88	93.5	98.3	101.3
Tensile strength, Rm, Mpa	64.3	81.2	94	106.3	120.1	142
Thermal conductivity (K)	212	217	320	356	392	421

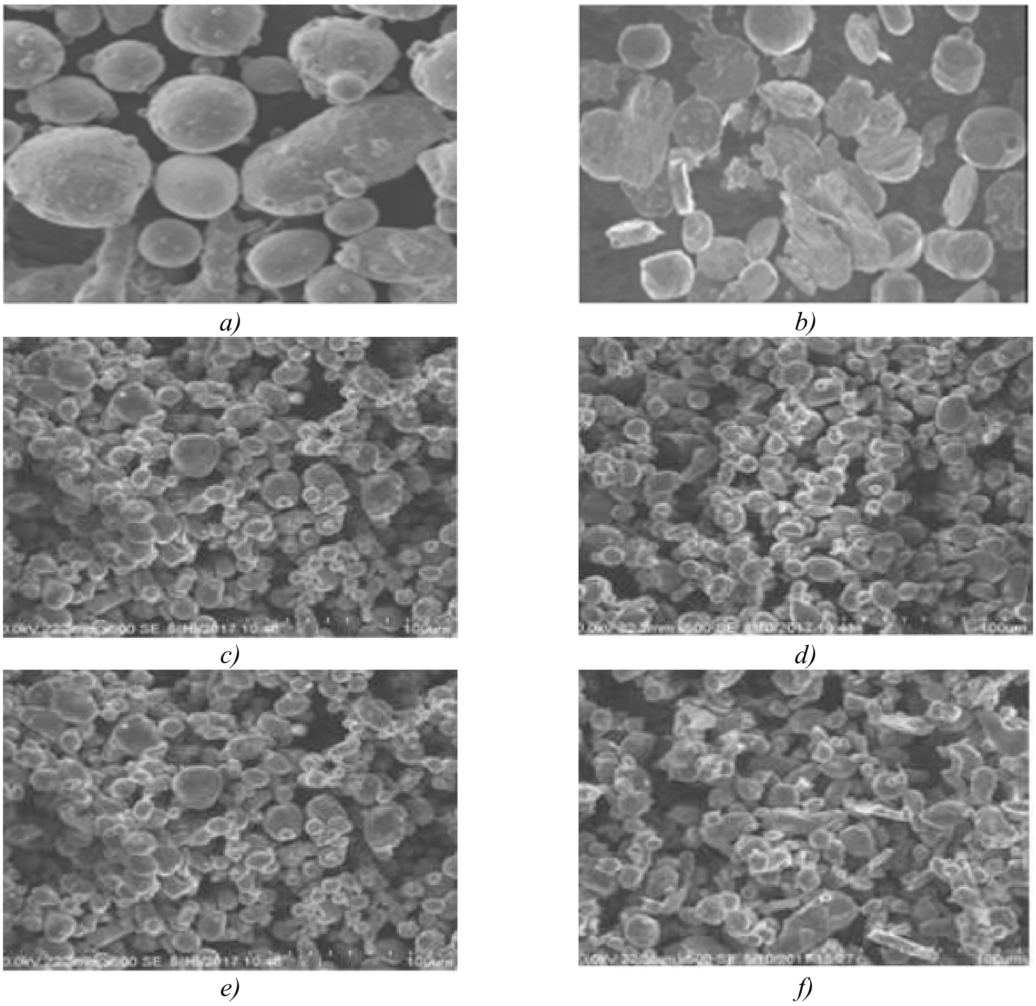

Fig. 2. FESEM images of Al+Grsample Grain Size with different Ratio magnification: a) 5:1 Magnification, b) 6:1 Magnification, c) 7:1Magnification , d) 8:1 Magnification , e) 9 Magnification 9:1, f) 10: 1Magnification

Figures 2. a to 2f show composite grain size magnification and grain size variability. This study, and examined pure aluminium pellets and aluminum-graphene composites with 0.25, 0.75, 1.0, 1.5,2.5,3.5,4.5, and 5.5 wt.% Gr metal matrix. Figures 1 and 2 show the Al-Gr composite fabrication schematics methodology and grain formation with ball milling. Figures 2(a)- 2 .f show raw aluminium and graphene composite morphological and chemical features (d). Hydraulic-crimped sintered Al-graphene pellets are used [1]. Predicted and selected suitable vacuum sintered temperature at 630°C for two hours at 5°C/min[1]. Al- Gr-based materials thermally fuse and predicted suitable temperatures. Hydraulic-crimped sintered Al-graphene pellets. Research-grade graphene and 99.9% pure aluminium powder were purchased. A suitable experiment was selected like 5-28 hours of 300-rpm high-energy ball milling. Milled aluminium composite powders were prepared and samples were developed by using methodology [1]. Experiments load like 1.28 tonne was compacted into 6 mm samples and 2.56 to 12.5 mm thickness samples were produced. Vacuum-sintering green pellets are used to conduct at 630 °C for two hours at 5 °C/min. Experimentally found that the Al-Gr-based compounds fused at this temperature.

3. Results and discussion

As stated in section 3.1 and further, [1] X-ray diffraction, FESEM, and microscopy were all investigated, and Raman and X-ray spectroscopy were employed to assess and compare the characteristics of composites. Through this study, pure aluminium and aluminum-graphene composite samples were analyzed, with graphene weight percentages ranging from 0.5 to 5.5 wt.% in the aluminium MMC (AlGr 0.5, 1.5, 2.5, 3.5, 4.5, and 5.5). Example procedures for creating Al-Gr composite samples by ball milling are shown in Figure 1[1][2]. Grain size changes from increased ball milling are shown in Figures 2(a) and 2(c), and the morphological and chemical assessments of a composite of virgin aluminium and graphene are shown in Figure 2. (d). Figure 2(a) and 2 show some representative FESEM images of Al and Al-Gr composites (with 1 to 5wt% graphene) (b). For thermal applications like heat sinks, it imports the Al-Graphene components that need to remain] [18].

3.1. X-ray diffractions for Al-Gr samples

. Figure 3. shows sample images of intensity concerning the 2θ and Raman shift of AlGr. It can be seen in the 0.25, 0.5, and 1wt% Gr. For all replicas (fresh Al and Al-Gr composites at 0.25, 0.5, 0.75, and 1 wt.%), X-ray diffraction peaks are shown in Figure 3. (a). Indicators of (111). For all models (fresh Al and Al-Gr composites at 0.25, 0.5, 0.75, and 1 wt.%), the X-ray diffraction peaks are shown in Figure 3. (a). Miller indices of (111), (200), and (220) are found in pure aluminium surfaces (311). Intensity is highest for aluminium and lowest for an Al-Gr composite containing just 1% graphene. Samples of Al-Gr composites are composed of high-crystalline aluminium material and ultra-compact graphene particles. The recognizable bands in graphene are seen in Fig. 3(b) (reduced graphene oxide). The D-band at 1300 cm^{-1} is chaotic because of defects, edge effects, and sp2 carbon bonds[1]. The 1580 cm1 G-band is formed by in-plane oscillations of sp2 hybridized carbon atoms. The Al-Gr compound remains uncontaminated because the G-band intensity is greater than the D-band. There is an improvement in the D- and G-bands of pure graphene samples[1].

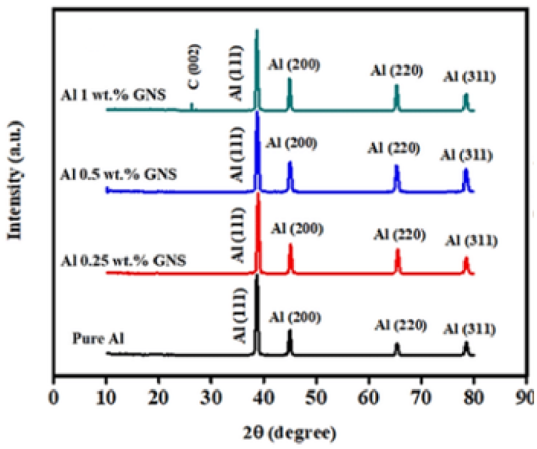

a)

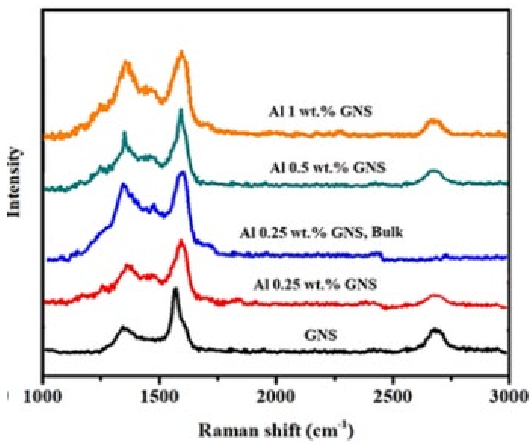

b)

Fig. 3. Sample Images of Intensity concerning 2theta and Raman shift:
a) X-ray intensity concerning 2theta b) Intensity concerning Raman Shift.

3.2. Examination of FESEM images

The primary goals of this study are to analyse the FESEM pictures of the Al-Gr (0.2 to 5 wt%) composite and to explore EDS. Figure 4 shows the FESEM images of grain reform with various duration of Ball milling. It can be seen grain reformed and fine size formation from Fig 4a to 4f was predicted using FESEM images. Grain size in typical Al-Gr (0.2 to 5 wt%) composites may be studied with the use of FESEM pictures, it varying from 20nm to 28nm. FESEM examination of the first and second phases reveals the Al and Gr grains before and during ball milling, as shown in Figs. 4b and 4d.

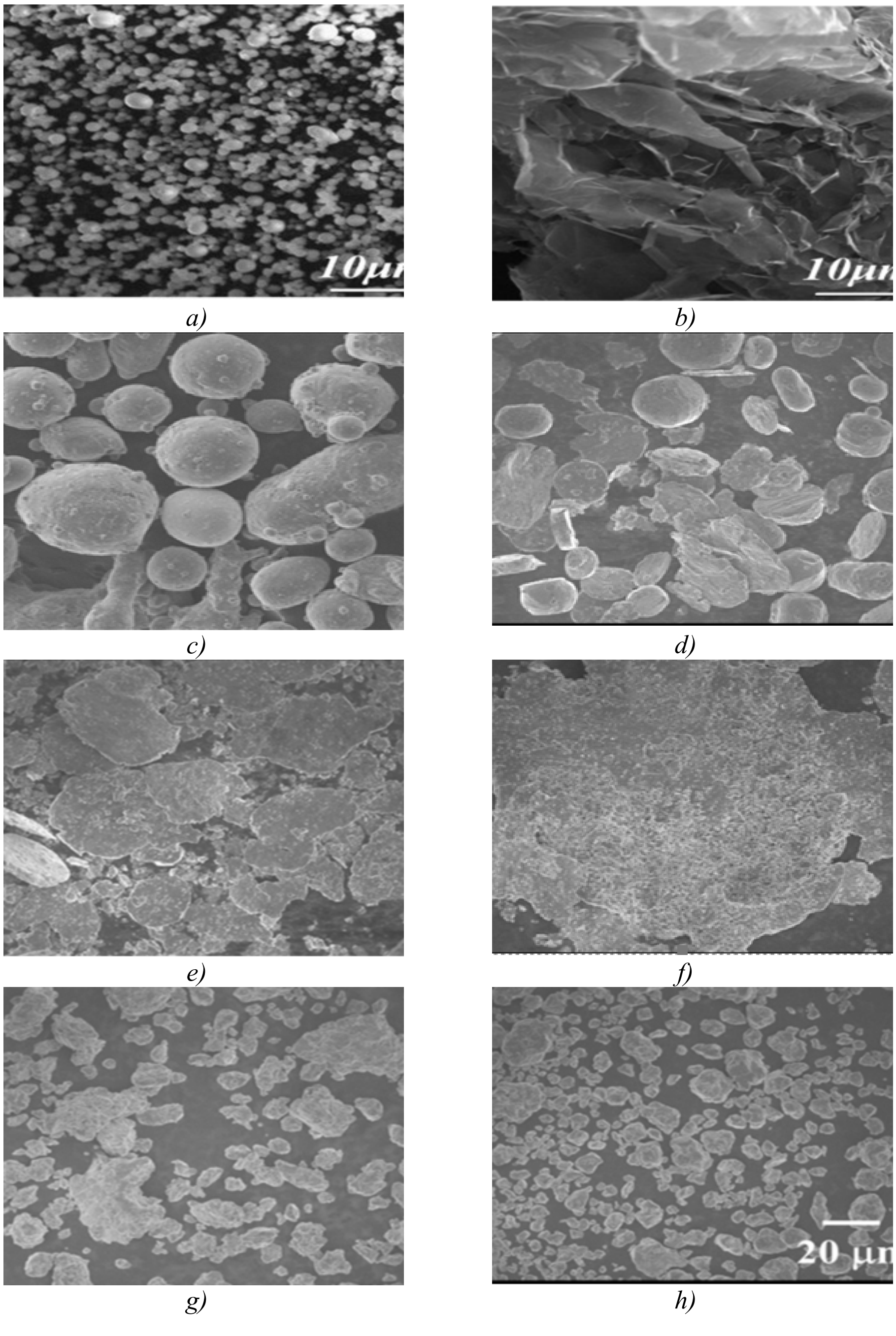

Fig. 4 FESEM Images of Al Graphen Composites after Ball Milling:
a) pure aluminum powder, b) Graphene, c) Al Graphene after 5 hours,
d) Al Graphene after 10 hours, e) Al Graphene after 15 hours, f) Al Graphene after 20hours,
g) Al Graphene after 24 hours,h) Al Graphene after 28 hours.

FESEM is a useful tool for inspection, and it has shown the absence of any pollutants. Microstructures observed with FESEM reveal layers and grain sizes characteristic of transparency-type graphene in Al-graphene (0.2 wt%) composites (Figure 4b). Aluminum powder with a density of 2.26 grams per cubic centimeter was used to create composites with a purity level of 99%. (Figures 4a-f). Several composite materials were produced by fixing the graphene percentage in the aluminium matrix[1]. The powder-to-filler ratio of 10:1 was used in a ball mill to ready the composite mixtures. Samples of pure Al and Al-Gr (0.2 wt%) composites were made by compacting at 120 MPa and sintering at 550 °C, as shown in Fig.4.a-f of the FESEM analysis. As can be seen in Fig. 4a, FESEM pictures of Al+Gr samples demonstrate their density and optimum compacted, as shown by the small grain size of the material.

3.3. EDS study with X-ray spectroscopy

Figure 5. a to 5. f shows some sample FESEM images of Al and GNPs and AL-GNPs. This FESEM and spectroscopy helped to identify the grain size and weight and % of atomic for different combinations and both EDS-analyzed and substance nature and X_ray Spectroscopy. X-rays affect samples of the particles. Atomic structure determines an element's electromagnetic emission spectrum [2]. (spectroscopy fundamentals) Moseley's law predicts peaks better than EDX. EDS compound quantification. EDS sorts matter. X-ray excitation. Element electromagnetic emission spectra have various peaks [2]. (spectroscopy foundation) Moseley's law outperforms EDX at peak prediction.

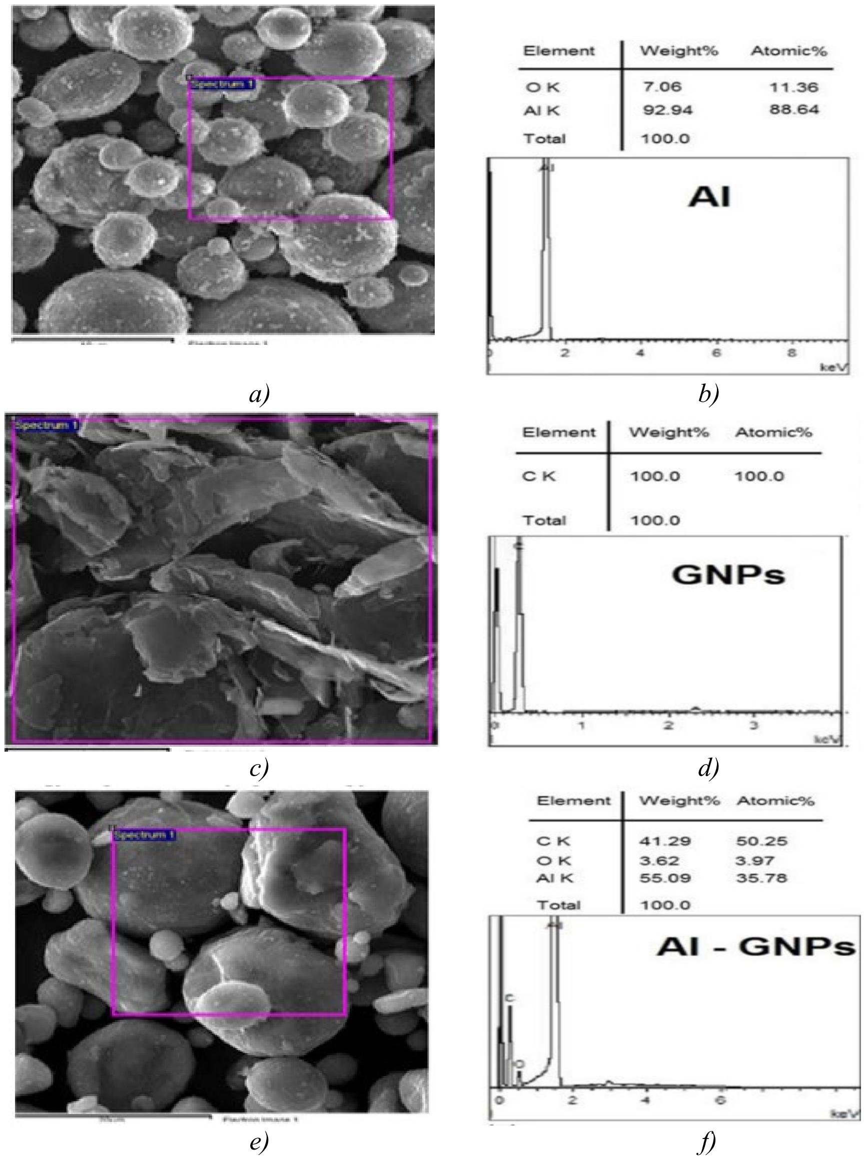

Fig. 5. FESEM Images and X-ray spectroscopy of Al, GNPs, and Al+GNPS:
a) FESEM Images of Al, b) X-ray Spectroscopy of Al, c) FESEM Images of GNPs,
d) FESEM Images of GNPs, e) FESEM Images of Al- GNPs, f) X-ray Spectroscopy of Al-GNP),

Figures 5a-5f show EDS estimations of chemical elements, multi-layer metallic coating thickness, and alloys. Quantitative sample composition studies are susceptible to confounding factors. Ti, V, Mn, Fe, and others have X-ray emission peaks. Sample type affects compositional estimation reliability. Laser-excited atoms produce X-rays. Radioactively-stable isotope X-rays. X-ray departure and detection depend on object composition, density, and energy. This and other X-ray absorption events need matrix adjustments to estimate sample composition from emission spectra. Composite structures and morphologies have been examined using X-ray diffraction, FESEM, energy-dispersive X-ray, and Raman spectroscopy. Sintered composites have 97.5% aluminium density. Micro-CT X-ray investigation revealed nonporous, structurally sound materials. Al-based composites have greater thermal conductivity and can sustain temperatures up to 630 °C without losing strength. These investigations suggest using Al-Gr composites as solar thermal collectors and heat sinks. Figure 5 shows energy-dispersive X-ray spectroscopy of pure aluminium and aluminum-graphene (0.1-0.3 wt%) composites compressed to 120 MPa and sintered at 550 °C. peak Al plane orientations (111), (200), and (311). Metal-graphene alloys. The graphene peak at C has 2 theta 26.5°, as we found [38]. (002). Al-graphene peaks (0.2 wt%) are frequent.

3.4. Raman spectroscopy

Raman spectroscopy is a method of non-destructive chemical examination that may provide knowledge about a substance's molecular interactions, crystalline nature, phase, and polymorphism. It relies on the way light reacts with a substance's chemical connections.

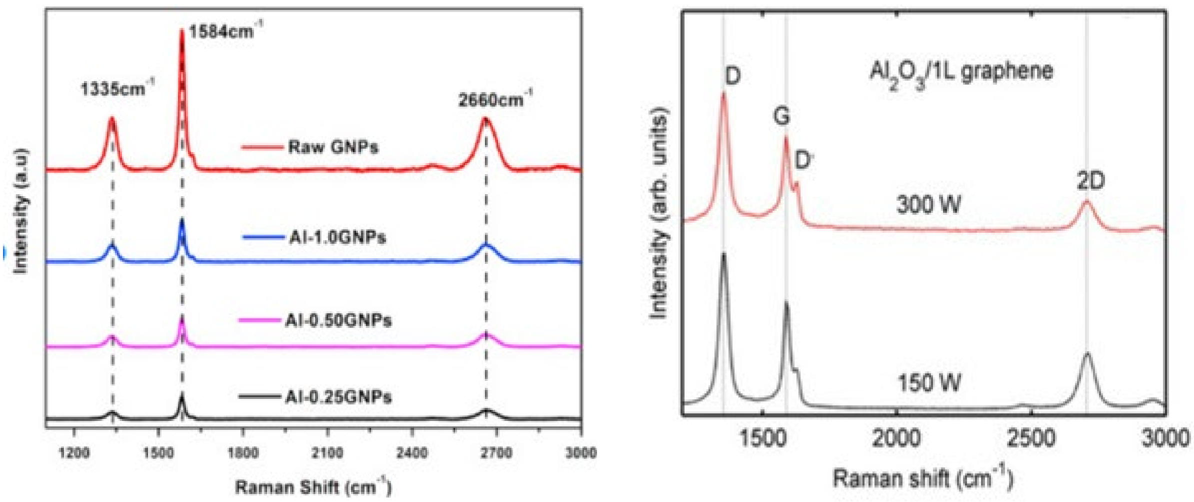

a) *b)*

Fig. 6. Raman Spectroscopy Images of the Raw GNPs Intensity Vs Raman shift:
a) Raman Spectroscopy Images of raw GNPs Vs Raman Shift,
b) Raman Spectroscopy for Intensity vs Raman Shift.

Figure 6. a 6. b shows Raman Spectroscopy analysis of AL+Gr composites it helps to find some properties like intensity. The intensity fluctuation associated with the Raman shift is seen in Figures 6. a and 6. b. One possible explanation is just because graphene is present in very small quantities in the Al-Gr composition. Spectroscopy is a quick method for providing clear input into electro-phonon exchanges due to its extraordinary sensitivity to electronic and crystallographic structures [2,5]. Raman spectra of carbon compounds exhibit three main bands between 1200 and 2800 $cm^{-1.}$ Raman spectra of both raw GNPs and physically disturbed composite powders. It's due to the disorder introduced by flaws in the graphitic materials used to make computers[1]. Positioned about in the center of the Scattering zone, the E2g photon has a frequency of around 1584 cm^{-1} or the G band. The 2D band at around 2700 cm -1 is the most reliable indicator of graphene's presence. G band shape, position, and intensity are all affected by the number of layers. In the Raman spectrum, the D, G, and 2D peaks stand out. Raman spectra of GNPs and physically agitated composite powders spread over SiO2 substrate showed a D band at 1335 cm -1, a significant G band at 1584 cm -1, and broad 2nd order 2D band at 2660 cm -1. Both the intensity and Raman intensity variation at different peaks like D and G are shown in Figures 6a and 6b. Graphene in the Al-Gr composite maintains its original characteristics since the G-higher band is stronger than the D-band[2][1]. Instead of being narrow as they are in pure graphene, the D and G bands are large and fuzzy. The Al-Gr composite could have some traces of graphene.

3.5. Thermal Conductivity Vs. wt% of Graphene

Figures 7 show the variation of Thermal conductivity concerning wt% of Gr. It can be seen that thermal conductivity increases with increasing the wt% of Graphene. At ambient temperature, Al-Gr composite with 1% graphene filler has 280 W/mK thermal conductivity, greater than virgin Al (124 W/mK)[1]. X-ray diffraction, FESM images, energy-dispersive X-ray spectroscopy, Raman spectroscopy, and others have examined composite structures and morphologies that helped in the analysis of the property Al+Gr. [1][2]. Sintering retained 97.5% aluminium density. X-ray micro-computed tomography indicated non-porous, structurally intact materials. [1][2]. 630 °C-fused Al-based composites are robust and 125% more thermally conductive than virgin Al.

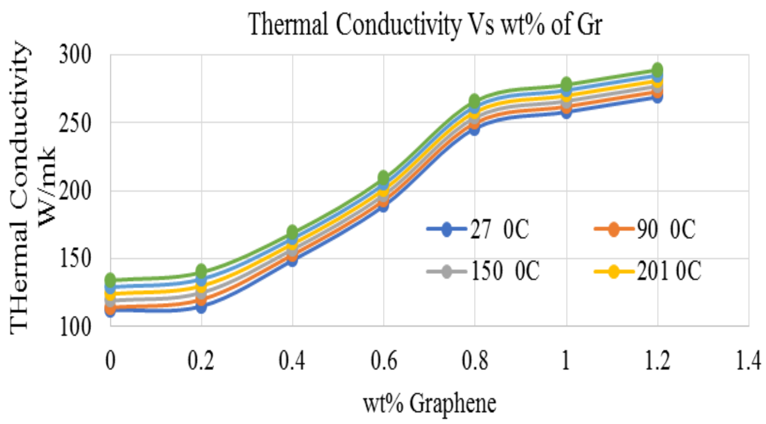

Fig 7 Thermal Conductivity vs. wt% of Graphene at various temperatures with1 to 1.2 wt% Graphene)

Figure 7 indicates the variation of 0 to 1.2 wt% of Gr and Figures 8 shows the compressive stress variation vs. compressive strain variation of the Al-Gr composite [1][2]. Sintering retained 97.5% aluminium density. X-ray micro-computed tomography indicated non-porous, structurally intact materials. [1][2]. 630 °C-fused Al-based composites are robust and 125% more thermally conductive than virgin Al.

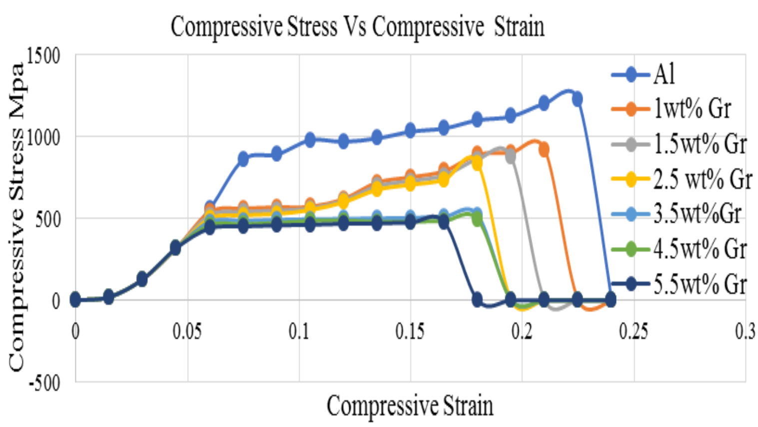

Fig. 8 Variation of Compressive Stress Vs. Compressive Strain comparison

Al with Gr composites widely used to develop solar thermal collectors and heat sinks. Fig. 8 exhibits Compressive Stress concerning compressive strain and it can be seen that Figure 7 shows the conductivity of an aluminum-graphene composite with varying graphene weight percentages. Maxwell, Russell, and Son-Frey match experimental values better than parallel. Russell's cubic Al matrix matches graphene's cubical array above 0.8% weight. 46[8]. Lower graphene volume percentages are directly proportional upto 0.05 wt%. Maxwell and Son-theories Frey fit experimental data for 0.6% weight fractions but diverge at higher fractions [6]. Filler particles form a continuous conducting network at high graphene levels but disperse at lower volume fractions. Multiple-concentration models fit experimental data[1].

a)

b)

c)

d)

e)

f)

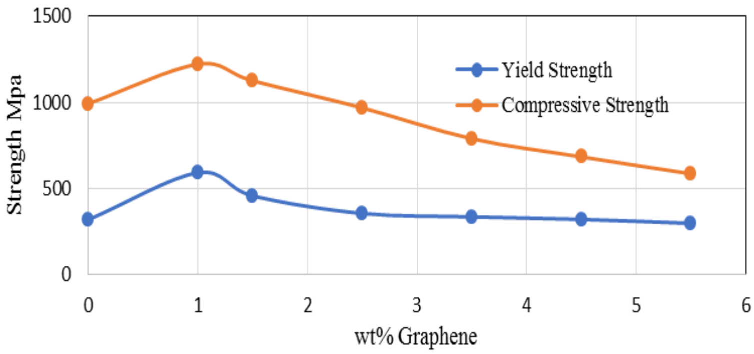

g)

Fig. 9. TensilerTest samples and Variation of Compressive Stress and Yield Strength Vs wt% Graphene: a)Tensile Strength test 1.5wt% of Gr, b)Tensile Strength test 2.5wt% of Gr, c)Tensile Strength test 3.5wt% of Gr, d)Tensile Strength test 4.5wt% of Gr, e)Tensile Strength test 5.0wt% of Gr.f)Tensile Strength test 2.5wt% of Gr, g) 9. g) Compressive and Yield strength Vs variation of Wt% of Gr

Fig. 9. Shows that Tensile test samples and 9. g exhibits the variation of compressive and yield strength concerning the variation of wt% of Gr. It helps to analyze and selects the suitable wt% of thermal collectors. The thermal heat conductivity of an aluminum-graphene composite with varying graphene weight percentages but compressive and yield strength decreases when increasing the wt % of Gr. At 1 wt% of Gr, the yield strength went up from 102 Mpa to 1325 Mpa,

while it went down from 1250 Mpa to 512 Mpa. When increasing the wt% of Gr from 1% to 5%, the compressive strength declined from 515 Mpa to 321 Mpa, and the yield strength followed this pattern. The temperature of the sintered samples was measured using a thermocouple. Mechanical stability under thermal stress and MMC are both heavily dependent on the thermal expansion coefficient [1]. Based on Experimental results and some authors like Maxwell, Russell, and Son-Frey matches experimental values better than parallel. Russell's cubic Al matrix matches graphene's cubical array above 0.8% weight. 46. Lower graphene volume percentages. Maxwell and Son-theories Frey fit experimental data for 0.6% weight fractions but diverge at higher fractions. Filler particles form a continuous conducting network at high graphene levels but disperse at lower volume fractions. Multiple-concentration models fit experimental data[1].

3.6. Micro-hardness

Figures 10 and 11 and 12 indicate that in hardness, Stress vs Strain comparison, and coefficient of thermal expansion Comparision plotted when the wt% of Gr is increased, the strength, yield, and compressive strength all fall significantly, whereas the microhardness first rises and then declines. At 1 wt% of Gr, the hardness value was 150 HV; when the wt% of Gr was increased, the hardness value dropped until it reached only 98.16 HV at 5.5 wt% of Gr, very near to the hardness values of the substrate.

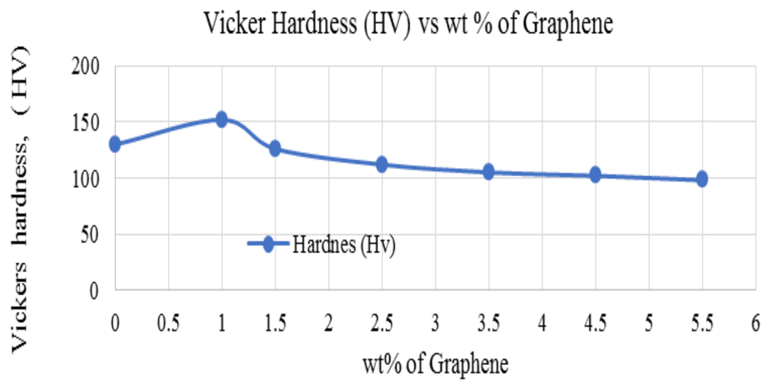

Fig. 10 Vicker Hardness (HV) Vs variation of Wt% of Gr

Figure 10 shows the comparison of Vicker's hardness concerning the variation of wt % of Gr as seen in Figure. Figure 8 shows that the Al-Gr composite material contains uniformly distributed spherical particles with a size range of 10-15 nm (b). Figure 10 illustrates the fluctuation of the coefficient of thermal expansion significantly increased from 5.36 to 26.56 /0C. Figure 8C demonstrates that the thermal expansion of composites is lower than that of composites with low wt% Gr compared to different temperatures. This study aids in the forecasting of various composites' hardness, thermal expansion, yield strength, and compressive. This research indicates a little reduction in strength, but an increase in conductivity, which is beneficial for thermal applications such as heat sinks. When comparing sintered pure Al (36 VHN) to sintered Al+Gr (0.25 wt%), the latter has a higher hardness (41 VHN).

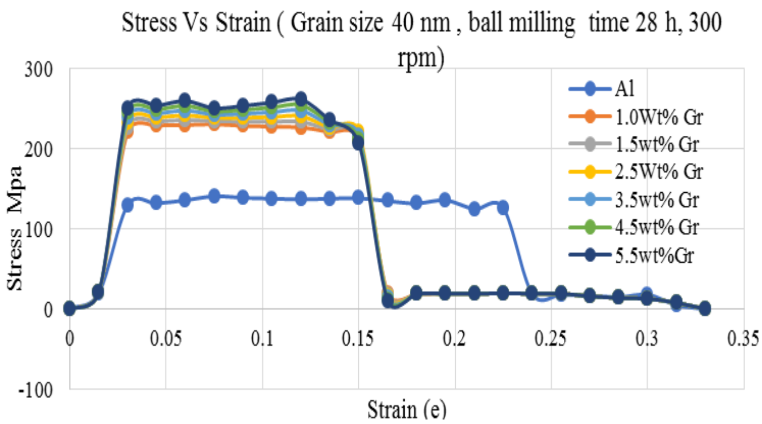

Fig.11 Stress vs Strain comparison concerning different wt% of Gr (1 to 5.5wt%)

Figure 11 shows the variation of stress-strain variation concerning various wt% Gr. The Al+Gr specimen under test is shown in Figure 11 According to tests, tensile strength drops as wt% of Gr content increases, and this trend holds over a range of Gr content percentages. The composite's working environment, condition, and materials all have a role in determining the composite's coefficient of thermal expansion. The Al-graphene composites were shown to be less brittle than pure Al across a wide range of temperatures [Figs. 4(a) and 4(b)]. Specifically, the coefficient of thermal expansion has a negative relationship with both the melting point and the adhesion strength [2].

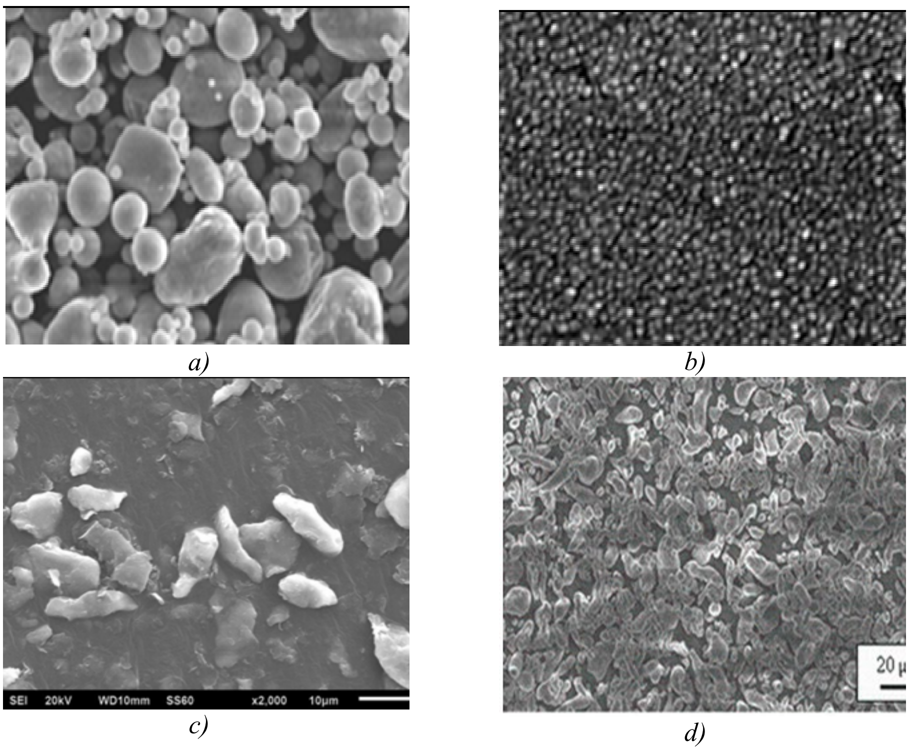

a) b) c) d)

Fig. 12. FESEM for Al+Grcomposites before and after ball milling:
a) Al+Grcomposites before Ball Milling. b) Gr before ball Milling,
c)) Al+Gr Composites with 4 wt % Gr after Ball milling with 20 hours,
d) Al+Gr Composites with 4 wt % Gr after 28 hours.

Figures 12. a to12. d shows some FESEM images for analyzing the grain size reformation and composites bonding during the ball milling process. It helps to demonstrate powder metallurgy composites. Al + graphene weight rose from 0.25 to 5% during powder metallurgical milling. Experimentally, its heat conductivity is 125% higher than metal. Al+ graphene increased room-temperature thermal conductivity from 0.25 to 1%. Pure and graphene-infused aluminium llosesheat conductivity over 300 degrees Celsius. (Fig. 5). (a). Thus, samples have a higher thermal conductivity at normal temperatures than at raised temperatures. Pure aluminium has 120 W/mK thermal conductivity. [1][2] [3]. FESEM images of composites at different Gr wt% helped determine grain and quality. Ball milling swiftly oxidizes aluminium into minute grains, reducing heat conductivity. (b). This research shows that adding wt% graphene to pure aluminium improves heat conductivity. Table I shows Al-Gr composite thermal dissipation's cost-effectiveness. Conventional mixing models for Al-Gr metal matrix composites analyzed all samples. Al-Gr with 5.5% graphene has 410 W/mK, greater than copper and aluminium. Supplements benefit health. X-ray micro-computed tomography investigated AlGr 5.5wt%'s three-dimensional morphology without damaging it (Bruker, Belgium). Figures 10. a -d show FESEM images of dispersive grains and particles and X-ray spectroscopy and analysis of Al+Gr (5.5 wt%). Figure 10 illustrates the three-dimensional morphology and grain structure of Al+Gr [1, 2, 3]. Aluminum and Gr in the basic Al matrix are homogeneous. Aluminum and carbon are equally dispersed, making graphene in the primary Al matrix homogeneous[1][10][3].

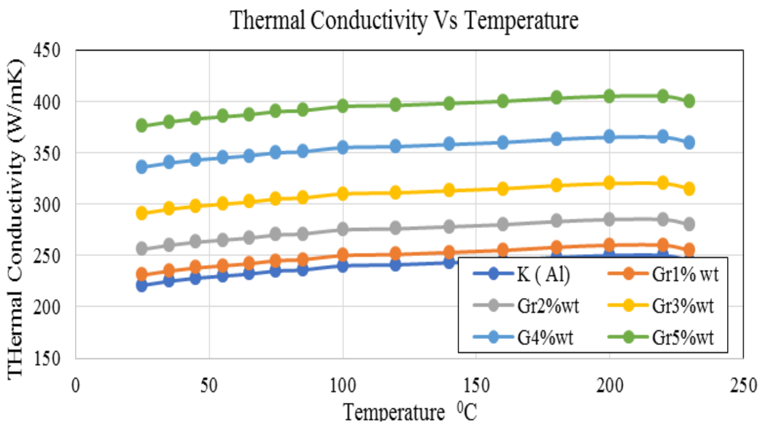

Fig. 13. Thermal Conductivity (W/mK) comparison vs. variation of Temperature (℃).

Figure 13 shows the thermal conductivity variation with temperature-dependent. Fig. 13 shows graphene-weighted aluminum-graphene composite thermal conductivity predictions and measurements for a range of graphene weight percents (wt%). The predicted values for spherical graphene fillers match the data for low wt% Gr concentrations but diverge considerably for higher-weight fractions [1]. An AMMC with a shape coefficient of 2.08 nm should evenly distribute fibres of different lengths in three dimensions. The composite's quality depends on the aspect ratio, surface-to-volume ratio, and Gr filler dispersion pattern[1][2]. Al-graphene composites have greater thermal conductivity than pure aluminium at various temperatures. Copper is a heat-absorbing foundation material for solar thermal collectors, but thermal applications need a metal with strong thermal conductivity [1, 2]. The main objective was to fabricate and evaluate the conductivity of five-cylinder-shaped aluminium castings doped with one to five percent graphene. This composite may lower solar thermal conductor prices. Simulations limit filler particle volume to 25%. This study only replicates AlGr composites since filler particles increased from 1% to 5%

wt% of Gr. Alternative filler particles may simulate composites without thermal barriers. Al-Gr composites with graphene up to 5.5wt% in the aluminium MMC has a thermal conductivity of 410 W/mK at 5wt% of Gr.

4. Conclusion

Powder metallurgy and a metal matrix composite (MMC) approach are utilized to create high-quality aluminum-graphene composites to enhance the economic viability of heat collectors. The following conclusions may be drawn from these experiments: grain size and a combination of thermal expansion relative to pure Al (124 W/mK) are both significantly reduced after sintering, and 97.5% of the original densities of the composite are conserved. Samples' structural integrity and lack of porosity were shown by FESEM pictures and Tomography. In comparison to pure aluminium, Al-Gr-based MMC composite materials were fused at 630 degrees Celsius and offered good strength and enhanced heat conductivity by 125%. Al+Gr composites are suitable for some solar thermal systems, for both the collectors and the heat sinks.

The Al+Gr composite materials, as determined by FESEM and spectroscopic analysis, included uniformly distributed spherical particles measuring 10–20 nm in size, and they generated superior samples of Al+Graphene.

The homogeneous distribution of elements in the Al and Gr composites that were used in the analysis and development of acceptable Ultra composites was made possible by the findings of experiments, FESEM, and some spectroscopy. The thermal conductivity of Al-Gr with 5.5% graphene has been predicted to be 410 W/mK, greater than that of copper and aluminium, while appropriate composites have been mostly made of Cu or aluminium and conduct 237 W/mK for current solar thermal collector applications.

Compared to pure Al and Cu, Al-Gr composites exhibited a greater thermal conductivity (410 W/mK). The resilience of Al-graphene composites to thermal stress has been shown experimentally to be greater than that of fresh-sintered Al. In a 3D aluminium cube matrix, discrete Gr is enclosed like MMC. The fibres would be randomly dispersed in all three spatial dimensions using a matrix with a shape coefficient of 2.08.

Acknowledgments

Coimbatore Institute of Technology, Coimbatore-14, India particularly Dr. A.S. Krishnan, Associate Professor, Dr. N.Rajamramasamy, Head of the Department of Mechanical Engineering, Dr. A. Rajeswari, Principal, and Dr. V. Selladurai, Adviser, has been extremely helpful and supportive throughout this project.

References

[1] M. Velliangiri, M. Karthikeyan, G. Suresh Kannan. ” vol. 20, no. 10, pp. 6229–6246, 2022, doi: 10.14704/NQ.2022.20.10.NQ55618.

[2] L. A. Yolshina, R. V. Muradymov, D. I. Vichuzhanin, E. O. Smirnova, AIP Conf. Proc., vol. 1785, no. November 2016; https://doi.org/10.1063/1.4967150

[3] S. K. Pradhan et al., AIP Adv., vol. 10, no. 6, 2020; https://doi.org/10.1063/5.0008786

[4] P. Garg, P. Gupta, D. Kumar, O. Parkash, J. Mater. Environ. Sci., vol. 7, no. 5, pp. 1461-1473, 2016.

[5] T. Sivaraman, V. Narasimhan, V. S. Nagarethinam, A. R. Balu, Prog. Nat. Sci. Mater. Int., vol. 25, no. 5, pp. 392-398, 2015; https://doi.org/10.1016/j.pnsc.2015.09.010

[6] A. Ibrahim, A. Klopocinska, K. Horvat, Z. A. Hamid, Graphene-Based Nanocomposites: Synthesis, Mechanical Properties, and Characterizations, 2021; https://doi.org/10.3390/polym13172869

[7] W. Ming Tian, S. mei Li, B. Wang, X. Chen, J. Hua Liu, M. Yu, Int. J. Miner. Metall. Mater., vol. 23, no. 6, pp. 723-729, 2016; https://doi.org/10.1007/s12613-016-1286-0

[8] S. Kumar and A. K. Mishra, Mechanical & Tribological Behaviors of Aluminium Metal Matrix / Hybrid Metal Matrix Composites : A Review, vol. 7, no. 15, pp. 1015-1032, 2020.

[9] S. Suresh, G. H. Gowd, M. L. S. D. Kumar, Adv. Compos. Hybrid Mater., vol. 2, no. 3, pp. 530-539, 2019; https://doi.org/10.1007/s42114-019-00101-y

[10] O. Guler, N. Bagci, J. Mater. Res. Technol., vol. 9, no. 3, pp. 6808-6833, 2020; https://doi.org/10.1016/j.jmrt.2020.01.077

[11] A. Saboori, M. Pavese, C. Badini, P. Fino, Acta Metall. Sin. (English Lett., vol. 30, no. 7, pp. 675-687, 2017; https://doi.org/10.1007/s40195-017-0579-2

[12] S. F. Bartolucci et al., Mater. Sci. Eng. A, vol. 528, no. 27, pp. 7933-7937, 2011; https://doi.org/10.1016/j.msea.2011.07.043

[13] J. Su, J. Teng, Front. Mater. Sci., vol. 15, no. 1, pp. 79-97, 2021; https://doi.org/10.1007/s11706-021-0541-0

[14] F. Chen, N. Gupta, R. K. Behera, P. K. Rohatgi, Jom, vol. 70, no. 6, pp. 837-845, 2018; https://doi.org/10.1007/s11837-018-2810-7

[15] X. Du, K. Zheng, F. Liu, Mater. Technol., vol. 52, no. 6, pp. 763-768, 2018; https://doi.org/10.17222/mit.2018.021

[16] A. Sharma, V. M. Sharma, J. Paul, J. Compos. Mater., vol. 54, no. 1, pp. 45-60, 2020; https://doi.org/10.1177/0021998319859427

[17] X. Zhang, S. Wang, Nanomaterials, vol. 11, no. 3, pp. 1-16, 2021; https://doi.org/10.3390/nano11030738

[18] R. T. Mousavian, J. Xu, X. Zhang, D. Gong, Compos. Part A Appl. Sci. Manuf., vol. 68, pp. 155-163, 2014; https://doi.org/10.1016/j.compositesa.2014.10.010

[19] S. Varghese, Int. J. Mech. Prod. Eng., no. 2, pp. 2320-2092, 2014.

[20] D. Pinto, A. Professor, Int. J. Innov. Sci. Res. Technol., vol. 2, no. 12, pp. 285-289, 2017, [Online]. Available: www.ijisrt.com.